JCI The Journal of Clinical Investigation

# Distinct interferon signatures and cytokine patterns define additional systemic autoinflammatory diseases

Adriana A. de Jesus, … , Scott W. Canna, Raphaela Goldbach-Mansky

*J Clin Invest.* 2019. https://doi.org/10.1172/JCI129301.

Clinical Research and Public Health | In-Press Preview | Immunology | Inflammation

## Graphical abstract

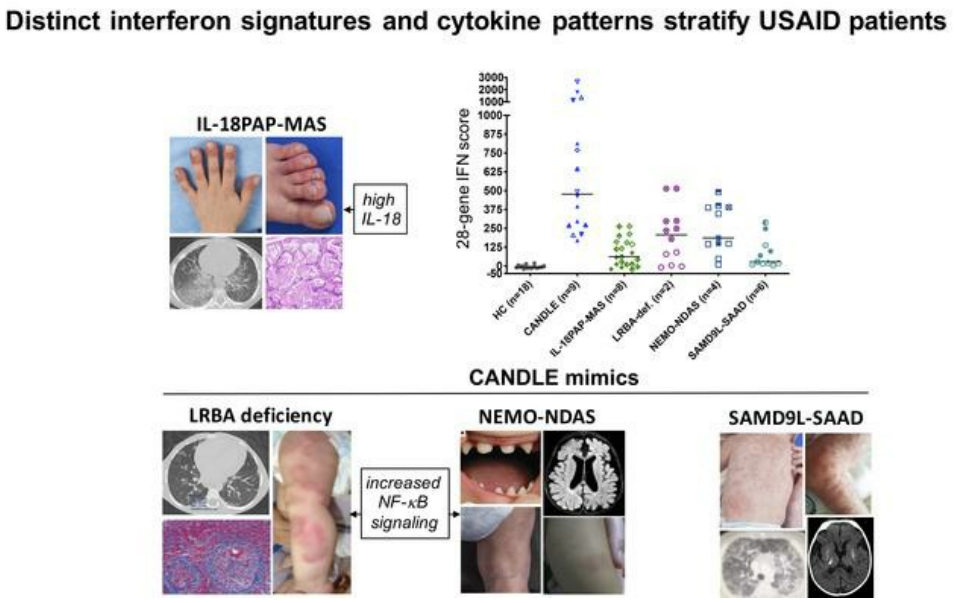

# Distinct Interferon Signatures and Cytokine Patterns Define Additional Systemic Autoinflammatory Diseases

**Short title:** IFN signature in undifferentiated immune-dysregulatory diseases

**Key words:** Autoinflammatory interferonopathies, undifferentiated autoinflammatory diseases blood interferon response gene score, macrophage activation syndrome

Adriana A. de Jesus, M.D., Ph.D.[1], Yangfeng Hou, M.D.[2], Stephen Brooks, Ph.D.[3], Louise Malle, B.S.[4], Angelique Biancotto, Ph.D.[5], Yan Huang, M.D., Ph.D.[1], Katherine R. Calvo, M.D., Ph.D.[6], Bernadette Marrero, Ph.D.[7], Susan Moir, Ph.D.[8], Andrew J. Oler, Ph.D.[9], Zuoming Deng, Ph.D.[3], Gina A. Montealegre Sanchez, M.D., M.S. [1], the Autoinflammatory Diseases Consortium (Amina Ahmed[10], Eric Allenspach[11], Bita Arabshahi[12], Edward Behrens[13], Susanne Benseler[14], Liliana Bezrodnik[15], Sharon Bout-Tabaku[16], AnneMarie C. Brescia[17], Diane Brown[18], Jon M. Burnham[13], Maria Soledad Caldirola[15], Ruy Carrasco[19], Alice Y. Chan[20], Rolando Cimaz[21], Paul Dancey[22], Jason Dare[23], Marietta DeGuzman[24], Victoria Dimitriades[25], Ian Ferguson[26], Polly Ferguson[27], Laura Finn[28], Marco Gattorno[29], Alexei A. Grom[30], Eric P. Hanson[31], Philip J. Hashkes[32], Christian M. Hedrich[33], Ronit Herzog[34], Gerd Horneff[35], Rita Jerath[36], Elizabeth Kessler[37], Hanna Kim[38], Daniel J. Kingsbury[39], Ronald M. Laxer[40], Pui Y. Lee[41], Min Ae Lee-Kirsch[42], Laura Lewandowski[43], Suzanne Li[44], Vibke Lilleby[45], Vafa Mammadova[46], Lakshmi N. Moorthy[47], Gulnara Nasrullayeva[46], Kathleen M. O'Neill[31], Karen Onel[48], Seza Ozen[49], Nancy Pan[48], Pascal Pillet[50], Daniela G.P. Piotto[51], Marilynn G. Punaro[52], Andreas Reiff[53], Adam Reinhardt[54], Lisa G. Rider[55], Rafael Rivas-Chacon[56], Tova Ronis[57], Angela Rösen-Wolff[42], Johannes Roth[58], Natasha Mckerran Ruth[59], Marite Rygg[60], Heinrike Schmeling[14], Grant Schulert[30], Christiaan Scott[61], Gisella Seminario[15], Andrew Shulman[62], Vidya Sivaraman[63], Mary Beth Son[64], Yuriy Stepanovskiy[65], Elizabeth Stringer[66], Sara Taber[67], Maria Teresa Terreri[51], Cynthia Tifft[68], Troy Torgerson[11], Laura Tosi[69], Annet Van Royen-Kerkhof[70], Theresa Wampler Muskardin[71]), Scott W. Canna, M.D.[72], Raphaela Goldbach-Mansky[1] M.D., M.H.S.

[1]Translational Autoinflammatory Diseases Section (TADS), NIAID/NIH, Bethesda, Maryland, United States
[2]Department of Rheumatology, Shandong Provincial Qianfoshan Hospital, Shandong University, Shandong, China
[3]Biomining and Discovery Section, NIAMS/NIH, Bethesda, Maryland, United States
[4]Icahn School of Medicine at Mount Sinai, New York, New York, United States
[5]Immunology & Inflammation Research Therapeutic Area, Sanofi, Boston, Massachusetts, United States

[6]Department of Laboratory Medicine (DLM), Clinical Center/NIH, Bethesda, Maryland, United States
[7]Computational Systems Biology Section, NIAID/NIH, Bethesda, Maryland, United States
[8]Laboratory of Immunoregulation, NIAID/NIH, Bethesda, Maryland, United States
[9]Bioinformatics and Computational Biosciences Branch (BCBB), Office of Cyber Infrastructure and Computational Biology (OCICB), NIAID/NIH, Bethesda, Maryland, United States
[10]Levine Children's Hospital, Charlotte, North Carolina, United States
[11]Divisions of Immunology & Rheumatology, Department of Pediatrics, University of Washington and Seattle Children's Hospital, Seattle, Washington, United States
[12]Virginia Commonwealth University & Pediatric Specialists of Virginia, Fairfax, Virginia, United States
[13]Division of Rheumatology, Children's Hospital of Philadelphia and the Perelman School of Medicine at the University of Pennsylvania, Philadelphia, Pennsylvania, United States
[14]Department of Pediatrics, Pediatric Rheumatology Section, Alberta Children's Hospital, University of Calgary, Calgary, Alberta, Canada
[15]Immunology Unit, Pediatric Hospital R. Gutierrez, Buenos Aires, Argentina
[16]Department of Pediatric Medicine, Sidra Medicine, Qatar Foundation, Doha, Qatar
[17]Nemours/Alfred I. DuPont Hospital for Children, Wilmington, Delaware, United States
[18]Division of Rheumatology, Children's Hospital Los Angeles & University of Southern California, Los Angeles, California, United States
[19]Pediatric Rheumatology, Dell Children's Medical Center of Central Texas, Austin, Texas, United States
[20]Divisions of Pediatric AIBMT & Rheumatology, University of California San Francisco, San Francisco, California, United States
[21]Department of Clinical Sciences and Community Health, University of Milano, Milan, Italy
[22]Division of Rheumatology, Janeway Children's Hospital & Rehabilitation Centre, Saint John's, Newfoundland and Labrador, Canada
[23]Division of Pediatric Rheumatology, University of Arkansas for Medical Sciences, Arkansas Children's Hospital, Little Rock, Arkansas, United States
[24]Department of Immunology, Allergy and Rheumatology, Baylor College of Medicine, Houston, Texas, United States
[25]Division of Pediatric Allergy, Immunology & Rheumatology, University of California Davis Health, Sacramento, CA, United States
[26]Department of Pediatrics/Pediatric Rheumatology, Yale University School of Medicine, New Haven, Connecticut, United States
[27]Pediatrics Department, University of Iowa Carver College of Medicine, Iowa City, Iowa, United States
[28]Pathology Department, University of Washington and Seattle Children's Hospital, Seattle, Washington, United States
[29]Center for Autoinflammatory Diseases and Immunedeficiencies, IRCCS Giannina Gaslini, Genoa, Italy

[30]Division of Rheumatology, Children's Hospital Medical Center, Cincinnati, Ohio, United States
[31]Department of Pediatrics Indiana University School of Medicine and Riley Hospital for Children, Indianapolis, Indiana, United States
[32]Pediatric Rheumatology Unit, Shaare Zedek Medical Center, Jerusalem, Israel
[33]Department of Women's & Children's Health, Institute of Translational Medicine, University of Liverpool & Department of Paediatric Rheumatology, Alder Hey Children's NHS Foundation Trust Hospital, Liverpool, United Kingdom
[34]Department of Otolaryngology, Division of Allergy and ImmunologyNew York University, New York, New York, United States
[35]Asklepios Klinik Sankt, Augustin GmbH, St. Augustin, Germany and Department of Pediatric and Adolescents Medicine, University of Cologne, Cologne, Germany
[36]Augusta University Medical Center, Augusta, Georgia, United States
[37]Division of Rheumatology, Children's Mercy, Kansas City and University of Missouri, Kansas City, Missouri, United States
[38]Pediatric Translational Research Branch, NIAMS/NIH, Bethesda, Maryland, Unite States
[39]Randall Children's Hospital at Legacy Emanuel, Portland, Oregon, United States
[40]Division of Pediatric Rheumatology, University of Toronto and The Hospital for Sick Children, Toronto, Ontario, Canada
[41]Division of Allergy, Immunology and Rheumatology, Boston Children's Hospital, Boston, Massachusetts, United States
[42]Department of Pediatrics, Medizinische Fakultät Carl Gustav Carus, Technische Universität Dresden, Dresden, Germany
[43]Systemic Autoimmunity Branch, NIAMS/NIH, Bethesda, Maryland, United States
[44]Hackensack University Medical Center; Hackensack Meridian School of Medicine at Seton Hall University, Hackensack, New Jersey, United States
[45]Department of Rheumatology, Pediatric Section, Oslo University Hospital, Oslo, Norway
[46]Azerbaijan Medical University, Baku, Azerbaijan
[47]Rutgers- Robert Wood Johnson Medical School, New Brunswick, New Jersey, United States
[48]Division of Pediatric Rheumatology Weill Cornell Medicine & Hospital for Special Surgery, New York, New York, United States
[49]Hacettepe University, Department of Pediatrics, Ankara, Turkey
[50]Children Hospital Pellegrin-Enfants, Bordeaux, France
[51]Department of Pediatric Rheumatology, Federal University of Sao Paulo, Sao Paulo, Brazil
[52]Department of Pediatrics, University of Texas Southwestern Medical Center, Dallas, Texas, United States
[53]Division of Rheumatology, Children's Hospital Los Angeles, Keck School of Medicine, USC, Los Angeles, California, United States
[54]University of Nebraska Medical Center/Children's Hospital and Medical Center, Omaha, Nebraska, United States
[55]Environmental Autoimmunity Group, NIEHS/NIH, Bethesda, Maryland, United States

[56]Department of Pediatric Rheumatology, Nicklaus Children's Hospital, Miami, Florida, United States
[57]Division of Pediatric Rheumatology, Children's National Health System, Washington, District of Columbia, United States
[58]Division of Pediatric Dermatology and Rheumatology, Children's Hospital of Eastern Ontario, Ottawa, Canada
[59]Medical University of South Carolina, Charleston, South Carolina, United States
[60]Department of Clinical and Molecular Medicine, NTNU - Norwegian University of Science and Technology, and Department of Pediatrics, St. Olavs Hospital, Trondheim, Norway
[61]University of Cape Town, Red Cross War Memorial Children's Hospital, Cape Town, South Africa
[62]Pediatric Rheumatology, Children's Hospital of Orange County, University of California Irvine, Irvine, California, United States
[63]Section of Rheumatology, Nationwide Children's Hospital, Columbus, Ohio, United States
[64]Division of Immunology, Boston Children's Hospital, Boston, Massachusetts, United States
[65]Department of Pediatric Infectious Diseases and Immunology, Shupyk National Medical Academy for Postgraduate Education, Kiev, Ukraine
[66]IWK Health Centre, Dalhousie University, Halifax, Nova Scotia, Canada
[67]Division of Pediatric Rheumatology, Department of Rheumatology, Hospital for Special Surgery, New York, New York, United States
[68]Undiagnosed Diseases Program, NHGRI/NIH, Bethesda, Maryland, United States
[69]Bone Health Program, Children's National Health System, Washington, District of Columbia, United States
[70]Department of Pediatric Immunology and Rheumatology, Wilhelmina Children's Hospital Utrecht, Utrecht, Netherlands
[71]New York University School of Medicine, New York, New York, United States
[72]Children's Hospital Pittsburgh, Pittsburgh, Pennsylvania, United States

Correspondence to:

Adriana A. de Jesus
adriana.almeidadejesus@nih.gov
Translational Autoinflammatory Diseases Section (TADS)/LCIM/ NIAID
NIH, Building 10 Room 11C215 MSC 1888
10 Center Dr.
Bethesda, MD 20892-1888
Phone: 301 761-7768

or

Raphaela Goldbach-Mansky
goldbacr@mail.nih.gov
Translational Autoinflammatory Diseases Section (TADS)/LCIM/ NIAID
NIH, Building 10 Room 11C205 MSC 1888
10 Center Dr.
Bethesda, MD 20892-1888
Phone: 301 761-7553

Trial registration: ClinicalTrials.gov NCT02974595

Funding: This research was supported by the Intramural Research Program of the NIH, NIAID, NIAMS and the Clinical Center.

Disclosures: RGM received investigator-initiated grants under government collaborative agreements from SOBI, Lilly, Regeneron and Novartis, outside the submitted work. SWC received grants from Novartis, Inc. and AB2Bio, Ltd., outside the submitted work. JAD received grants from Pfizer, Roche and Bristol-Myers Squibb, outside the submitted work. AAG received grants from NovImmune, grants and personal fees from Ab2Bio, during the conduct of the study; and grants from Novartis, outside the submitted work. RML received consultant fees from SOBI and Novartis, outside the submitted work. LGR received research support from Hope Pharmaceuticals, Bristol Myers Squibb and Elli Lily, outside the submitted work. GS received personal fees from Novartis, outside the submitted work. TLWM received grants from Arthritis National Research Foundation, NYU Clinical & Translational Science Institute, during the conduct of the study; personal fees from Novartis, outside the submitted work; and has a patent Methods and Materials for Treating Autoimmune Conditions issued.

**Abstract (251)**

*Background.* Undifferentiated systemic autoinflammatory diseases (USAID) present diagnostic and therapeutic challenges. Chronic interferon (IFN) signaling and cytokine dysregulation may identify diseases with available targeted treatments.

*Methods.* Sixty-six consecutively-referred USAID patients underwent standardized evaluation of Type-I IFN-response-gene-signature (IRG-S); cytokine profiling, and genetic evaluation by next-generation sequencing.

*Results.* Thirty-six USAID patients (55%) had elevated IRG-S. Neutrophilic panniculitis (40% vs 0%), basal ganglia calcifications (46% vs 0%), interstitial lung disease (47% vs 5%), and myositis (60% vs 10%) were more prevalent in patients with elevated IRG-S. Moderate IRG-S elevation and highly-elevated serum IL-18 distinguished eight patients with pulmonary alveolar proteinosis (PAP) and recurrent macrophage activation syndrome (MAS). Among patients with panniculitis and progressive cytopenias, two patients were compound heterozygous for novel *LRBA* mutations, four patients harbored novel splice variants in *IKBKG/*NEMO, and six patients had *de novo* frameshift mutations in *SAMD9L.* Of additional 12 patients with elevated IRG-S and CANDLE-, SAVI- or Aicardi-Goutières-Syndrome (AGS)-like phenotypes, five patients carried mutations in either *SAMHD1, TREX1, PSMB8 or PSMG2*. Two patients had anti-MDA5 autoantibody-positive juvenile dermatomyositis, and seven could not be classified. Patients with *LRBA, IKBKG/NEMO* and *SAMD9L* mutations showed a pattern of IRG elevation that suggests prominent NF-κB activation different from the canonical interferonopathies CANDLE, SAVI and AGS.

*Conclusions.* In patients with elevated IRG-S, we identified characteristic clinical features and 3 additional autoinflammatory diseases: IL-18-mediated PAP and recurrent MAS (IL-18PAP-MAS), NEMOΔ5-associated autoinflammatory syndrome (NEMO-NDAS), and SAMD9L-associated autoinflammatory disease (SAMD9L-SAAD). The IRG-S expands the diagnostic armamentarium in evaluating USAIDs and points to different pathways regulating IRG expression.

## INTRODUCTION

The discovery of Mendelian defects that cause immune-dysregulatory and autoinflammatory diseases rapidly expanded our ability to diagnose pediatric patients with systemic sterile inflammation and provided insights into pathogenic mechanisms that cause organ inflammation and damage. Furthermore, pathogenesis and treatment studies in autoinflammatory diseases converge on confirming a key role of proinflammatory cytokines in amplifying abnormal immune responses, which have become effective targets for treatments (1).

Mutations in IL-1 activating inflammasomes (including the NLRP3 and pyrin) and their remarkable response to IL-1 inhibiting therapies suggested a central role of IL-1 to their pathogenesis (1). More recently, two diseases with systemic inflammation, one caused by gain-of-function mutations in the viral sensor *TMEM173*/STING causing STING-associated vasculopathy with onset in infancy (SAVI) and another by additive loss-of-function mutations in proteasome genes causing the Proteasome-Associated Autoinflammatory Syndromes (PRAAS) (also: chronic atypical neutrophilic dermatosis with lipodystrophy and elevated temperatures, CANDLE), presented with chronically elevated interferon (IFN) signatures, implicating a pathogenic role of Type-I IFN in autoinflammatory diseases (2, 3). Type-I IFN was first discovered as a soluble anti-viral factor over 50 years ago, and a role in sterile inflammation was proposed in patients with systemic lupus erythematosus (4). However, the discovery of genetic mutations that cause the autoinflammatory Type-I interferonopathies CANDLE (2, 5), SAVI (3, 6-8) and Aicardi Goutières syndrome (AGS) (9, 10) have shed light on pathomechanisms that drive chronic IFN signaling and recent studies blocking IFN signaling validate a critical role of Type-I IFNs (11). AGS-causing loss-of-function mutations in nucleases impair self-nucleic acid homeostasis, SAVI-causing gain-of-function mutations in *TMEM173* lead to chronic predominantly IFN-$\beta$ production and PRAAS-causing loss-of-function mutations in proteasome genes cause an elevated IFN-signature that is independent of nucleic acids

and viral sensor activation and points to additional intracellular mechanisms that trigger an IFN-signature.

A link between autoinflammation and Type-II IFN (IFNγ) was recently established via the discovery of gain-of-function mutations in *NLRC4* (12, 13). Patients demonstrate chronically and extremely high levels of serum IL-18, as well as evidence for IFNγ activity during flares (14). Highly elevated serum IL-18 levels emerged as risk factors for developing macrophage activation syndrome (MAS) and have been associated with the development of MAS in systemic juvenile idiopathic arthritis and adult onset Still's disease (15, 16). The disease-causing *NLRC4* mutations have associated the NLRC4 inflammasome but not the other inflammasomes to very high IL-18 activation (15). Mutations in *XIAP* (17) and *CDC42* (18) are other monogenic autoinflammatory syndromes with high IL-18 levels that predispose to the development of MAS, thus providing genetically-defined disease models to study the role of IL-18 in MAS. The presence of free IL-18 in these patients with ultrahigh serum IL-18 level may modify the synergy with IL-12 in promoting the production of the Type-II IFN, IFNγ (19), which emerges as the critical factor in promoting the hyperinflammatory state of MAS (14).

Emerging data from interventional studies targeting the Type-I IFN and IL-18/Type-II IFN pathways have shown benefit in patients with these diseases and treatment might benefit patients who currently have no genetic diagnosis but evidence of immune dysregulation in the respective inflammatory pathways. Patients with high IFN-signatures may clinically respond to treatments that block Type-I IFN-signaling (11). Likewise, patients with high serum IL-18 levels and a MAS predisposition might respond to treatments that target IL-18 (20) and/or the Type-II IFN, IFNγ (21).

Comprehensive clinical phenotyping of USAID patients and screening by assessing the IFN signature, a targeted cytokine profile and by genomic evaluation, led to the identification of three additional autoinflammatory diseases, IL-18-associated pulmonary alveolar proteinosis (PAP) and MAS syndrome (IL-18PAP-MAS), NEMOΔ5-associated autoinflammatory syndrome (NEMO-NDAS), and SAMD9L-associated autoinflammatory disease (SAMD9L-SAAD). The preferential elevation of IRGs with STAT-1 and NF-κB

binding sites in patients with NEMO-NDAS, LRBA deficiency and SAMD9L-SAAD suggests a prominent role of both NF-κB and IFN signaling distinct from CANDLE, SAVI and AGS.

**RESULTS**

**Interferon score screening identifies distinct clinical features in patients with elevated Interferon response gene score (IRG-S) compared to patients with normal IRG-S.**

IRG expression is low in healthy controls and untreated patients with the IL-1-mediated disease, neonatal-onset multisystem inflammatory disease (NOMID) and elevated in patients with PRAAS/CANDLE and SAVI were assessed. Of 65 patients tested for IRG-S elevation (see workflow in Figure 1), 36 (55%) had elevated IRG signatures with an active disease flare and 29 patients were negative (Figure 2A). Four of the 29 patients with a normal IRG-S at the time of testing were later included in one of the disease groups of patients with an elevated IRG-S during disease flares (Table 1 and Supplemental Table 1). Clinical and laboratory features varied in patients with and without elevated IRG-S and a significantly earlier disease-onset was observed in patients with elevated IRG-S (Figure 2B-G, Table 1 and Supplemental Table 1). Panniculitis was present in 22 patients (54%) included in disease groups with an elevated IRG-S, compared to no patient with a normal IRG-S (*p<0.0001*). Similarly, basal ganglia calcifications were present in 12 out of 26 patients (46%) with elevated IRG-S who had either CTs or MRIs compared to none of 14 patients with normal IRG-S (*p<0.01*). Other clinical features that were more frequent in patients with elevated IRG-S included interstitial lung disease (47% vs. 5% in patients with normal IRG-S), myositis (60% vs. 10% with normal IRG-S), arterial hypertension (30% vs. 4% with normal IRG-S), and liver enzyme elevation (61% vs. 12% with normal IRG-S) (Table 1).

On laboratory evaluation (Supplemental Table 2), lymphopenia (with low B cell and NK cell counts) and thrombocytopenia were present in 24-31% of patients with elevated IRG-S compared to none with normal IRG-S; patients with high IRG-S were more frequently anemic (36% vs 8%). Antinuclear antibodies (ANA) were present in patients with and without IRG signature (33% vs. 11%, (p=ns)) but were more prevalent in patients with an elevated IRG-S; anti-dsDNA antibodies and anti-neutrophil antibodies (anti-PR3

and anti-MPO) were low positive in 1 or 2 patients with an elevated IRG-S each. In contrast, autoantibodies to endothelial lipoproteins (anti-cardiolipin, lupus anticoagulant) were equally positive in patients with and without elevated IRG-S. Serum IgA and IgM levels were higher in patients with elevated IRG-S (Supplemental Table 2).

Mortality within the period of the study was high in patients with positive IRG-S; 8 /41 (19.5%) expired within the period of this study (2014 to 2018); all patients with normal IRG-S are alive (Table 1). The analyses focused on characterizing patients with elevated IRG-S, in whom the IRG-S elevation was associated with active disease, although absence of infection could not always be excluded as contributing factor.

Of the 41 patients in the disease groups with elevated IRG-S, 18 were diagnosed with additional diseases based on clinical phenotype, cytokine and/or genetic analyses and are described in groups 1 to 4 (G1-G4). Eight patients with PAP and recurrent MAS were grouped into Group 1 (G1). Twelve patients with CANDLE-like features had relatively lower IRG-S with disease flares and were later genetically classified with distinct diseases: LRBA deficiency (G2, n=2), NEMO-NDAS (G3, n=4) and SAMD9L-SAAD (G4, n=6). Several patients with high IRG-S resembled AGS (G5, n=4) and one of them had a known mutation in *SAMHD1*. Two patients with high IRG-S scores, interstitial lung disease, soft tissue calcifications, and myositis had elevated anti-MDA5 autoantibodies, consistent with anti-MDA5 autoantibody-positive juvenile dermatomyositis (JDM) (G6, n=2). Of the remaining patients in the disease groups with positive IRG-S, 3 had mutation-positive CANDLE and 3 had CANDLE-like features and were grouped in group 7 (G7, n=6). Of the 3 CANDLE patients one had a known mutation (n=1) one had a novel mutation in the CANDLE-causing gene, *PSMB8* (n=1) and one patient was compound heterozygous for mutations in a novel CANDLE-causing gene (n=1). Two patients with SAVI-like features were without disease-causing mutations and are described in group 8, G8 (SAVI-like)(n=2) (see Supplemental Methods for definition of disease categories, Supplemental Methods A). Seven patients, each with clinical features unlike any other patient, could not be grouped or classified (G9, n=7).

We assessed 48 cytokines in 53 patients with available serum samples Supplemental Figure 1). The median IP-10 levels were significantly higher in patients with an elevated IRG-S (n=20) compared to those with a normal IRG-S (n=25) (7,369 (404.1 – 25,884) vs. 622.1 (191.4 – 3,185) pg/ml, *p<0.0001*). Other cytokines that were significantly elevated include MIG/CXCL9 (2,890 (441.9 – 43,205) vs. 737.5 (83.4 – 1,272) pg/ml, *p=0.0001*), SCF/KITLG (38.9 (4.3 – 209.8) vs. 20.9 (3.5 – 107.2) pg/ml, *p=0.0156*), GRO$\alpha$/CXCL1 (251.6 (74.9 – 1,696) vs. 161.7 (24.9 – 314.8) pg/ml, *p=0.0043*) and TRAIL (94.8 (18.1 – 633.3) vs. 47.9 (10.7 – 290.0) pg/ml, *p=0.0277*).

**Highly-elevated serum IL-18 levels, pulmonary alveolar proteinosis (PAP), and recurrent macrophage activation syndrome (MAS) characterize a defined clinical syndrome.**

Eight patients with a history of recurrent macrophage activation syndrome (MAS), pulmonary alveolar proteinosis (PAP) and nail clubbing (Figure 3A-C), had ultra-high elevations of serum IL-18 levels (Figures 3D and 3E). Three were repeatedly tested for the entire cytokine panel and had significantly increased expression of a 12-cytokine signature nearly identical to that seen in patients with an *NLRC4* gain-of-function mutation and recurrent MAS (NLRC4-MAS) which includes hematopoietic growth factors/cytokines like M-CSF, SCF, and IL-3 (12) (Figure 3D). However, whole exome sequencing did not reveal definitive candidate mutations and no patient had *NLRC4* mutations. The distinct clinical presentation with PAP, the very high IL-18 levels (Figure 3E), an IL-18/CXCL9 ratio similar to patients with NLRC4-MAS (14) (Figure 3F), and a cytokine signature previously associated with recurrent MAS clinically suggest a previously unrecognized disease, that is subsequently referred to as IL-18 associated PAP and MAS syndrome (IL-18PAP-MAS). Patients are combined in Group 1 (G1). Of the 8 patients, 7 patients had active disease at the time of assessment and 6 had an elevated IRG-S with active disease, although elevations were significantly lower than in CANDLE and SAVI (*p=0.0002 and p=0.0003* respectively) (Figure 4A)**.** In one patient with inactive disease and a normal C-reactive protein (CRP) at the time of blood draw, serum IL-18 levels had dropped from 430,423pg/ml during active disease to 2,506pg/ml

(normal<500pg/ml) and the IRG-S was normal. This patient was included in Group 1 (G1) due to the clinical phenotype of IL-18PAP-MAS and the ultra-high IL-18 levels at the time of active disease. Supplemental Table 3 includes the clinical features and treatments for the IL-18PAP-MAS group.

**Genetic analyses of 12 patients with CANDLE-like clinical phenotypes including panniculitis, but also progressive B cell lymphopenia, and low/intermediate IRG-S revealed novel mutations in *LRBA*, novel splice variants in *IKBKG*/NEMO, and truncating mutations in *SAMD9L*.**

Twelve patients with CANDLE-like phenotypes who were negative for known CANDLE-causing mutations had low/intermediate IRG-S and all developed progressive cytopenias. Whole exome sequencing (WES) identified 2 patients with novel or very rare compound heterozygous *LRBA* (LPS Responsive Beige-Like Anchor Protein) mutations (22). One of the LRBA-deficiency patients (G2-P2) had severe lipoatrophy, hepatomegaly, and Type 2 insulin-resistant diabetes (DM Type 2). A *de novo* mutation in *IRS1,* (c.3632T>G; p.L1211R) encoding the insulin receptor substrate 1 previously associated with DM Type 2 (23, 24) may have contributed to this phenotype but was not formally evaluated. Upon leptin replacement, the patient's profound insulin-resistant diabetes and hepatosplenomegaly resolved (25). The patient subsequently developed transverse myelitis and septic arthritis and underwent a bone marrow transplant. The other patient (G2-P1) had recurrent neutrophilic panniculitis in predominantly lower extremities and granulomatous hepatitis (Supplemental Table 4). Both patients were combined in Group 2 (G2) based on their biallelic *LRBA* mutations, reduced surface expression of CTLA4, and reduced number of regulatory T cells consistent with previous findings (26) (data not shown).

One patient with lymphohistiocytic panniculitis and chorioretinitis (G3-P1) had conical teeth reminiscent of the ectodermal dysplasia found in NEMO (NF-κB essential modulator) deficiency syndrome, which prompted targeted sequencing of *IKBKG*, (the causative gene in NEMO deficiency), the gamma subunit of the IκB kinase complex that

regulates NF-κB activation. This patient, 2 other males and one girl with panniculitis, progressive B-cell lymphopenia, and hypogammaglobulinemia all had *de novo* splice-site variants that lead to deletion of exon 5 of *IKBKG* (G3-P1 to P4) and are listed under Group 3 (G3) (Supplemental Table 4).

Genetic evaluation of 6 other patients revealed 3 tightly-clustered *de novo* frameshift mutations in *SAMD9L.* All patients were clinically diagnosed as CANDLE due to the prominent neutrophilic panniculitis that was clinically and histologically indistinguishable from CANDLE. However, four patients also had early-onset, severe interstitial lung disease, a clinical feature that is not seen in CANDLE (Figure 4B). These patients had lower IRG-S scores in the context of high CRPs and developed progressive isolated B cell and NK cell cytopenias (Supplemental Table 4). One patient, who succumbed from respiratory failure at the age of 2 months, was included post mortem; she and 2 other patients had the identical *de novo* frameshift mutations in *SAMD9L*. Two patients with *SAMD9L* mutations (G4-P1 and G4-P4) had elevated IRG-S scores. Of the other 3 patients tested, two (G4-P3 and G4-P5) had negative IRG-S and the third patient (G4-P2) had 4 samples tested, 3 with negative IRG-S, and 1 sample, obtained during a rhinovirus induced disease flare, had an elevated IRG-S. Two patients received bone marrow transplants, G4-P3 had received a sibling matched bone marrow transplant at the age of 20 months, a second patient (G4-P5) received an allogeneic bone marrow transplant at the age of 9 months.

The highly similar clinical presentation, progressive B cell lymphopenia, and genetic findings (frameshift mutations all within 13 AAs of each other, absent from public databases, and in a conserved protein domain) support their classification as a previously unrecognized autoinflammatory disease, referred to as SAMD9L-associated autoinflammatory disease (SAMD9L-SAAD) (G4) (Figure 4A-C and Supplemental Table 4).

**Novel and known mutations in PRAAS/CANDLE and AGS-causing genes characterize patients with high IRG-S scores and suggestive clinical features.**

Of 4 patients summarized in group 5 (G5) with neurologic disease manifestations, two had spastic quadriplegia and were wheelchair bound (G5-P2 and P3); patient 2 expired in the context of a presumed infection. One patient (G5-P1) who suffered a stroke at the age of 7 years had Moya-Moya like vasculopathy and was later found to have a previously-described (27) homozygous *SAMHD1* deletion. Patient G5-P3 had spastic quadriplegia and peripheral vasculitis. Her father was incidentally found to have a very high IRG-S score and extensive basal ganglia calcifications during workup of "muscle weakness" and included as a patient (G5-P4).

Two patients who suffered from digital ulcerations, interstitial lung disease and myositis were initially thought to have an autoinflammatory disease, but the presence of anti-MDA5 autoantibodies was consistent with a diagnosis of anti-MDA5 autoantibody-positive JDM. No obvious candidate gene was identified, and these patients (G6-P1 and P2) were grouped together in Group 6 (G6).

Six patients with CANDLE-like features, who had no cytopenias but high IRG-S, were included in Group 7 (G7). Of these, 3 had disease-causing CANDLE mutations (G7-P5 through P6). Patient G7-P4 was homozygous for a known *PSMB8* mutation (p.T75M). Patient G7-P5 was compound heterozygous for two novel *PSMB8* mutations (p.S118P and p.Q55*) and patient G7-P6 harbored novel compound heterozygous mutations in the proteasome assembly gene, *PSMG2*/PAC2 that were recently confirmed to be pathogenic (28). Patient G7-P3 had severe localized panniculitis, localized lipoatrophy, and basal ganglia calcifications without white matter disease, and harbored a *de novo* somatic mutation (~36% allele fraction) in *TREX1* that was previously associated with autosomal dominant Aicardi Goutières Syndrome 1 (AGS1) as a germline mutation (29). Four G7 patients (G7-P3, -P4, -P5 and -P6) were treated with JAK inhibitors with good responses. Patient G7-P4 died due to severe pulmonary hypertension, which developed prior to initiation of JAK inhibitor treatment (30). Two siblings, G7-P1 and -P2 have no genetic diagnosis. Group 8 (G8) includes two patients with SAVI-like disease (G8-P1 and G8-P2) who presented with chilblains lesions and systemic inflammation but carried no obvious candidate mutations (Table 2 and Supplemental Table 5).

In Group 9 (G9), 7 patients with elevated IRG-S scores who could not be grouped on clinical, immunological or genetic basis were described (Supplemental Table 6).

**IFN-score negative patients can be grouped according to clinical phenotype, genotype and cytokines profile**

The findings of the 25 patients with negative IRG-S scores are described in Supplemental Table 7. Patients could be classified into 4 subgroups: 5 patients had chronic recurrent multifocal osteomyelitis (CRMO) (GN1) n=5. GN1-P2 and GN1-P5 had exclusive jaw involvement and the others had long bone and spine involvement, no unifying genetic hypothesis was found. Four patients had cryopyrin-associated periodic syndrome (CAPS)- like disease (GN2) n=4. Interestingly, all had a rare variant of unknown significance in *NLRP3* that was inherited from a parent. All patients in GN2 had complete or partial responses to IL-1 blocking treatment, strengthening the concept that selected low-penetrance variants may predispose to the development of CAPS-like disease (31). No unifying genetic hypothesis was found for 6 patients with periodic fever syndromes (GN3) n=6. Three patients with systemic juvenile idiopathic arthritis (sJIA)-like disease and MAS (GN4) n=3 had all high serum IL-18 levels between 9,878 pg/mL and 24,200 pg/mL and IL-18/CXCL9 ratios >1 that have previously been associated with increased risk for the development of MAS (15). Seven patients could not be grouped (GN5) n=7.

**Distinct gene expression patterns in 3 NF-κB co-regulated IRGs distinguish disease groups with both, NF-κB and IFN signaling for potential leveraging of the diversity in IRGs regulation for diagnostic purposes.**

Though all disease groups had elevated IRG-S compared to negative controls (HC and NOMID), the mean IRG-S score elevation was significantly lower in patients with IL-18PAP-MAS (G1), LRBA deficiency (G2), NEMO-NDAS (G3) and SAMD9L-SAAD (G4). Normalized gene expression for 25 of the 28 ISGs in our assay was significantly higher in CANDLE, SAVI, and disease groups G5-G8 compared to groups G1-G4 except for normalized gene expression in 3 genes, *CXCL10, GBP1 and SOCS1,* which was equal or

higher in groups G2-G4 compared to CANDLE and SAVI (Supplemental Figure 2 and Supplemental Figure 3A).

We hypothesized that the differential expression of these genes may be due to regulation by different transcription factors (TF). We therefore assessed TF binding sites (TFBS) in the 28 genes in our IFN score. As expected, all 28 genes have TFBS for STAT1 and other TFs activated by Type-I IFNs. The 3 genes with relatively higher expression in patient groups G1-G4 compared to CANDLE and SAVI, have additional TFBS for either NF-κB1 (*CXCL10*, *GBP1* and *SOCS1*) and/or NF-κB2 (*CXCL10*) (Supplemental Figure 3B), thus suggesting that NF-κB-dependent activation of these IRGs may be relatively higher in patients in G1-G4 than STAT1-dependent activation which differs in patients with CANDLE and SAVI. To validate a role of NF−κB in driving their expression, we correlated the expression level of the 3 genes (*CXCL10*, *GBP1* and *SOCS1*) with that of 11 genes that have NF−κB but no STAT1 TFBS, by calculating summary z-scores, a "3-genes NF-κB/STAT1 score" and an "11-gene NF-κB-only validation score" (Supplemental Methods and Supplemental Figures 3 and 4). The 3-gene "NF-κB/STAT1 score" did not correlate with the "11-gene NF-κB-only validation score" in HCs who have no IFN score elevation nor in CANDLE, and SAVI, where we expected predominant Type-I IFN/STAT1 inflammation. However, the "11-gene NF-κB-only validation score" highly correlated with the "3-genes NF-κB/STAT1 score" in patients with LRBA deficiency (G2, r=0.82, *p=0.02*), NEMO-NDAS (G3, r=0.72, *p=0.03*) and SAMD9L-SAAD (G4, r=0.99, *p=0.002*) (Supplemental Figure 5). A "25-gene STAT1-only score" of genes expressing only STAT1 but no NF-kB TFBSs did not correlate with the 11-gene NF-κB-only validation score" in any disease group with elevated IRG-S. Interestingly, in the IL-18PAP-MAS patients, neither the "3-gene NF-κB/STAT1 score" nor the "25-gene STAT1-only score" correlated with the "11-gene NF-κB-only score" (G1) (Supplemental Figure 5B). TFs that are activated by recombinant IL-18 (including FOS, ATF2, JUN and ATF3) (32) were present in the regulatory domains of many of the IRGs in the 28-gene IRG-S (data not shown). In support of the notion that free IL-18 may co-regulate the expression of IRGs in patients with IL-18PAP-MAS, we correlated total serum IL-18 levels, which correlates with free IL-18 levels (15), with the

IRG-S and found that only serum levels of IL-18 but not IL-18BP and CXCL9 correlated weakly with the 28-gene IRG-S (r=0.3, p=0.06, Supplemental Figure 6A).

A ratio of the "3-gene NF-κB/STAT1 score" and the "25-gene STAT1-only score" (3/25 ratio) to reflect the relative contribution of NF-κB vs. STAT1/IFN mediated inflammation was very low in CANDLE, SAVI, AGS, AGS-like disease (G5), anti-MDA5 autoantibody-positive JDM (G6), CANDLE/CANDLE-like disease (G7), and SAVI-like disease (G8) (Figure 4A) as well as in childhood systemic lupus erythematosus (SLE) and other JDM (Supplemental Figure 7). A ratio less than 0.07 or greater than 0.15 or distinguished the canonical interferonopathies (SAVI or CANDLE) and patients with LRBA deficiency (G2) and with NEMO-NDAS (G3) from healthy controls and NOMID patients, respectively (Figure 4). The 3/25 ratio was normal in IL-18PAP-MAS. Interestingly, the ratio of IFNγ and IFNα regulated genes over all genes was higher in the IL-18PAP-MAS than in CANDLE and SAVI (Supplemental Figure 6B).

**Preliminary outcomes in patients who received treatment with a JAK inhibitor**

Although this study was not conducted to collect treatment outcomes, we report preliminary observations to increase available data on these very rare diseases to improve management (Supplemental Table 8). A total of 15 patients have received treatment with JAK inhibitors. Five patients received baricitinib in the context of a compassionate use study (NCT01724580), the other 10 patients received the JAK inhibitor through commercial sources; 7 received tofacitinib, 2 ruxolitinib and one baricitinib (Supplemental Table 8). Two patients expired during the period of this study, both received tofacitinib, one patient with anti-MDA5-antibody JDM, who received ruxolitinib while on a ventilator for worsening lung disease. The other patient, a CANDLE patient, had severe primary pulmonary hypertension prior to starting tofacitinib (30). One patient with a psoriasiform dermatitis and scarring Skin fibrosis, had no response to 9 months of treatment and discontinued baricitinib treatment (G9-P1). Two additional CANDLE patients (G7-P5 and G7-P6 (28) and one patient with CANDLE-like disease and a somatic *TREX1* mutation (G7-P3) had complete responses to JAK inhibition and continue on treatment. One patient

with AGS5 (G5-P1) was previously reported (33) and has stable disease on baricitinib. Two patients with AGS-like disease had partial to minimal responses to baricitinib and tofacitinib (G5-P3, P4) respectively with ongoing significant steroid requirement in one patient (G5-P3). Another patient with anti-MDA5 antibody-positive JDM (G6-P1) had a partial response to low dose of tofacitinib with progressive soft tissue and cardiac calcifications. Of the patients in G1-G4, the patient with IL-18PAP-MAS has a partial response with no progression of lung disease and decreasing serum IL-18 levels (G1-P7), the patient with the *LRBA* deficiency has had partial responses with resolving cytopenias and rashes, and lower steroid requirements (G2-P1). One patient with NEMO-NDAS (G3-P4) had a suboptimal response and discontinued tofacitinib; lastly one patient with SAMD9L-SAAD (G4-P1) has a partial response with ongoing skin disease and steroid requirements reported in (28). Based on our findings we suggest disease criteria to diagnose patients with and without IRG-S (Supplemental Table 9).

**Discussion**

Mendelian autoinflammatory interferonopathies present with chronic elevation of an IRG-S (summarized in (34)). Clinical benefit in patients treated with JAK inhibitors who have CANDLE (11), SAVI (11, 35, 36) or AGS (37, 38) are encouraging and the correlation of treatment responses with suppression of the IRG-S score (34), suggests the IRG-S score as useful in diagnosis and as a biomarker in monitoring treatment responses. In this study, a strategy for screening patients with undifferentiated autoinflammatory diseases that included assessment of IRG-S score, cytokine profiling, clinical phenotyping, and genomics led to characterization of additional disease groups of patients with both chronic and temporary IRG-S elevations and to the development of a ratio of differentially regulated IRGs that were included in a 28-gene score that distinguishes the additional conditions from the canonical interferonopathies, CANDLE, SAVI and AGS.

Compared to patients with a negative IRG-S, which included patients with osteomyelitis, CAPS-like disease, periodic fever syndromes and sJIA-like disease with MAS

flares and high IL-18 levels, most of which responded to IL-1 blocking treatments, patients with elevated IRG-S had more severe disease and higher mortality thus underlining the unmet need to find better treatments.

The characterization of patients with clinical phenotypes that resemble CANDLE/PRAAS, who had overall lower IRG-S and developed progressive B cell cytopenias and or hypogammaglobulinemia, led to the recognition of 3 distinct, monogenic conditions, that underline the importance of assessing these mutations in patients suspected to have CANDLE/PRAAS and who are negative for mutations in genes that encode proteasome components. Two patients with CANDLE/PRAAS-like phenotypes had loss-of-function (LOF) mutations in *LRBA* causing LRBA deficiency (39). Both patients (G2-P1 and G2-P2) had panniculitis and lower CTLA4 surface expression on CD4+ T cells than controls (data not shown), which confirm that the novel mutations impact CTLA4 recycling (26). However, both patients carry other mutations that may affect IFN signaling (Supplemental Table 4). It therefore remains to be determined whether the IFN signature is a characteristic part of the immune dysregulation of patients with LRBA deficiency (22) or is associated with other rare variants in LRBA deficiency. Patient G2-P1 is partially responding to JAK inhibition with concomitant decrease in IRG-S after previously unsatisfactory responses to sirolimus and abatacept (Supplemental Table 4), suggesting a possible pathogenic role of increased IFN signaling.

Four patients harbor novel splice variants in *IKBKG*/NEMO, the gamma subunit of the IκB kinase complex that activates NF-κB. In contrast to patients deficient in the NEMO protein who exhibit immunodeficiency, patients with the NEMO spliced mutant who lack only exon 5 (NEMOΔexon5) do not present with severe immunodeficiency but with systemic inflammation panniculitis and elevated IRG-S score. Hanson et al. recently explored the molecular mechanisms that coactivate NF-κB and IRGs in these patients and called the disease NEMO-NDAS and found that NEMOΔexon5 stabilizes the TBK1/IKKi complex and facilitates IRF3 phosphorylation, *IFNB1* transcription, and concomitant NF-κB activation. These evaluations provide a potential mechanistic explanation for the

Type-I IFN associated "autoinflammatory" clinical features and the concomitant NF-κB nuclear translocation in this previously unrecognized inflammatory syndrome (40).

A severe perinatal-onset inflammatory disease was seen in 6 patients with frameshift mutations in *SAMD9L* that is phenotypically distinct from two diseases previously associated with heterozygous missense mutations in *SAMD9L* (41-44). One of the diseases, pancytopenia and ataxia syndrome (41, 44), presents later in life with concomitant cerebellar atrophy and risk of myelodysplasia. Other somatic and selective germline *SAMD9L* mutations can cause pediatric early-onset myelodysplastic syndrome (MDS) (43). The six patients reported here harbor novel, *de novo* frameshift mutations that are in close proximity to each other. The mutations cause immune-dysregulation characterized by nodular panniculitis similar to CANDLE/PRAAS, and early-onset interstitial lung disease in most patients (unlike CANDLE/PRAAS), and severe infection-associated myelosuppression/cytopenias. Genetic reversion that is described in pancytopenia and ataxia syndrome (41) and in pediatric MDS (43) was also seen in one patient prior to bone marrow transplant. The inflammatory disease manifestations suggest that these heterozygous *SAMD9L* frameshift mutations confer a gain-of function (GOF) through mechanisms that need to be further investigated. Furthermore, the positive outcome of bone marrow transplantation in 2 of the 6 patients, and the high mortality in patients who have severe concomitant lung disease, point to the importance of distinguishing these patients from CANDLE by making the diagnosis of SAMD9L-SAAD early.

Eight patients uniformly presented with recurrent MAS-like episodes and developed PAP/lipoid pneumonia and clubbing of their distal phalanges. They were diagnosed clinically as a previously unrecognized disease that is referred to as IL-18PAP-MAS. These patients' histological findings of PAP are distinct from the interstitial fibrosis of SAVI, and are not seen in patients with NLRC4-associated MAS despite comparably high serum IL-18 levels (12, 15). Similarly, elevated IL-18 levels are also seen in some patients with sJIA and adult Still's disease, and are now recognized as factors predisposing to the development of MAS (15, 17, 45-47). Some of these patients are included in a publication

that highlights a larger spectrum of sJIA patients who develop a heterogeneous spectrum of lung diseases that include PAP and interstitial lung fibrosis and are referred to as sJIA-LD (48). Patients with IL-18PAP-MAS share a cytokine signature linked to high expression of IL-18 and originally described in NLRC4-MAS (12), which includes hematopoietic growth factors/cytokines like M-CSF, SCF, and IL-3. Interestingly, humanized mice with transgenic expression of human SCF, IL-3, and GM-CSF develop spontaneous MAS directly mediated by myeloid cells (49), raising questions whether IL-18 promotes the production of these growth factors. These mechanisms may synergize with the known function of the role of IL-18 as IFNγ-stimulating factor in infections and may provide further potential mechanisms by which IL-18 confers MAS susceptibility. The presence of PAP suggests alveolar macrophage dysfunction in clearing surfactant from the alveoli, as is seen in patients with genetic or autoimmune GM-CSF deficiency (50). Whether IL-18 blockade, IFNγ and/or treatments aimed at increasing surfactant phagocytosis/processing by alveolar macrophages are viable treatment strategies needs further exploration. Genetic analyses have so far not been conclusive in the IL-18PAP-MAS patients nor the other sJIA-LD patients (48).

Interestingly, the magnitude and pattern of the IRG elevation differed between these four conditions (LRBA deficiency, NEMO-NDAS, SAMD9L-SAAD and IL-18PAP-MAS) versus CANDLE and SAVI. The expression of 3 IRGs that contain both NF-κB and STAT1 TFBS (*CXCL10, GBP1* and *SOCS*1) correlated with IFN-independent NF-κB induced gene expression in LRBA-deficiency and NEMO-NDAS, and in SAMD9L-SAAD during flares when IRG-S scores were elevated, suggesting a relatively larger effect of NF-κB signaling, compared to the canonical interferonopathies (CANDLE, SAVI and AGS) and some autoimmune interferonopathies. Although preliminary, our data suggest that patients with IL-18PAP-MAS, LRBA deficiency, NEMO-NDAS and SAMD9L-SAAD may have more variable responses to JAK inhibition than CANDLE patients, consistent with the observation, that the inflammatory response is complex. The partial response to JAK inhibition would be expected in this scenario and may suggest treatment combination that target the IFN-mediated and NFkB-mediated dysregulation. In the IL-18PAP-MAS

patients IRGs induced by IFN-α and IFN-γ relative those induced by predominantly IFN-α were higher in IL-18PAP-MAS than in the other diseases. The pattern of IRGs did not correlate with NF-κB induced genes, but correlated weakly with the patients' highly elevated total serum IL-18 levels (often >200,000 pg/ml when normal levels are < 500 pg/ml) (15). As any of the IRGs in the 28-gene IRG-S have TFs in their respective regulatory domains that are activated by recombinant IL-18, the correlation of IL-18 levels with the IRG-S suggests that free IL-18 may co-regulate the expression of IRGs in patients with IL-18PAP-MAS. IL-18 induces IFNγ (51), which emerges as critical downstream mediator of the pathogenesis of MAS (15). Whether and how free IL-18 drives the IRG-S, directly via co-regulating expression of IRGs or via promoting IFNγ needs to be evaluated. Pathomechanisms underlying the promising results with JAK inhibition in MAS and hemophagocytic lymphohistiocytosis (HLH) (52-54) may be partially attributable to IFNγ receptor signaling blockade (21), but treatments targeting the IL-18/IFNγ axis are promising (55).

Overall, this study establishes the value of screening for an IFN signature and for high serum IL-18 levels and expands the diagnostic armamentarium that supports the challenging evaluation of patients with undifferentiated autoinflammatory diseases. The diagnosis of IL-18PAP-MAS, NEMO-NDAS, SAMD9L-SAAD and LRBA deficiency need to be considered in patients presenting with elevated IRG-S scores and clinically suggestive features. A high ratio of 3/25 differentially regulated interferon-response genes identified NEMO-NDAS, LRBA deficiency and a normal ratio the SAMD9L-SAAD patients. These diseases mimic CANDLE/PRAAS clinically but higher 3/25 ratios suggest relative a increased NF-κB signaling distinct from CANDLE/PRAAS and SAVI. Future investigations are necessary to determine whether the 3/25 ratio will be useful in predicting respond to IFN-targeted monotherapy, versus the need for additional treatments.

**Patients and Methods**

**Patients and healthy controls**. Between 2014 and 2017, 66 consecutive patients with presumed undifferentiated autoinflammatory diseases who had no genetic diagnosis

upon referral were included in an institutional review board (IRB) approved natural history study (NCT02974595). All clinical investigations were conducted according to Declaration of Helsinki principles. Written informed consent was obtained from the subjects or their parents either at the NIH or by phone consent. Blood samples were collected from patients and their unaffected family members when available. Healthy controls were recruited through the same study, NCT02974595, and were siblings or family members who have no mutations. For some assays anonymous healthy blood donors were used.

**Clinical, immunological, and genetic evaluation.** We assessed 57 patients at the NIH (including physical exam, clinically indicated imaging and a chest CT) and immunologically (T, B, NK cell count, immunoglobulins and rheumatologic work up). Five patients passed away before an NIH visit could be arranged, and in 4 patients logistical problems precluded travel to the NIH. Samples for genetic testing were obtained from all 66 patients either at the NIH or were sent under NCT02974595. Whole exome sequencing (WES) was performed in 19 trios, 1 duo and 4 singletons, whole genome sequencing (WGS) in 36 trios and 1 duo; 5 patients had Sanger sequencing of candidate genes performed only. Confirmatory targeted (Sanger) sequencing of candidate genes detected by WES or WGS was performed. Next-generation sequencing data are registered in dbGaP under accession number phs001946.v1.p1.

**Cytokine Analysis.** Serum was collected from 53 of 66 patients and 5 healthy controls. Cytokine concentrations of 48 analytes were measured using the Bio-Plex system (Bio-Rad, Hercules, CA)(3) in 2 batches. Cytokine analysis was done in 28 of the 36 patients with elevated IFN signature (UIFN). The first batch included 45 patients, 20 with UIFN and 25 without UIFN, and 5 healthy controls and the second batch included 8 patients with an UIFN. Due to a ceiling effect of high serum IL-18 levels in the Bio-Plex system, all samples with levels >10,000pg/ml were re-run in a dedicated ELISA assay as previously described

(15). All patients with a history of macrophage activation syndrome had serum measurements that included IL-18, IL-18BP and CXCL9 (MIG) as described in (15).

**Nanostring 28-gene IFN Response Gene Signature (IRG-S) Score.** At least one IRG-S score was obtained on 65 of 66 patients. It was not obtained from one patient with a *SAMD9L* mutation (G4-P5). As previously reported, total RNA was extracted from blood samples collected in Paxgene tubes (Qiagen, Hilden, Germany). Gene expression of selected IRGs was determined by Nanostring (NanoString Technologies, Seattle, WA) and an IFN-score was calculated as previously described based on healthy control data as described (34).

Within the 28 IRGs of the Nanostring IFN score, 3 IRGs were identified as having a *NFKB1* and/or a *NFKB2* TFBS. For validation and correlation of a 3-gene-subscore of IRGs with STAT1 and NF-κB1 and NF-κB2 transcription factor binding sites (TFBS) with other genes preferentially activated by NF-κB1 and NF-κB2 that lack STAT1 binding sites, please refer to Supplemental Methods D and Supplemental Figures 3B and 4A,B.

*Evaluation of the 3-gene to 25-gene ratio (3/25 ratio) in the various diseases:*

A ratio of the sum of the normalized counts of the 3 nanostring ISGs with NF-κB binding sites (*CXCL10*, *GBP1* and *SOCS1*) and the sum of the normalized counts of the 25 other genes was generated and compared between diseases.

**Statistical analysis**. Descriptive analyses were performed, no adjustments for multiple comparisons were made. For normally distributed data, parametric tests (unpaired 2-tailed t-tests for group comparison (i.e. cytokine analysis) were used. Non-parametric tests were used for not normally distributed data (Kruskal-Wallis for multiple comparisons and Mann-Whitney test for group comparison). Pearson correlation was used for correlations of the 3, 11 and 25-gene subscores. Receiver-operating characteristic (ROC) curves were generated comparing the 3-gene/25-gene ratio in CANDLE and SAVI vs. the various disease groups (G1-G9) to healthy controls (HC) and NOMID samples using the

Wilson/Brown method; a confidence interval of 95% is reported. P-value below 0.05 was considered statistically significant for all tests performed. All statistical analyses described above were performed using GraphPad Prism version 8.00 for macOS, GraphPad Software, La Jolla California USA, www.graphpad.com.

**Study Approval**

The study was approved by institutional review boards at the National Institutes of Health, NIAID. All patients were enrolled in the NIH Natural History Protocol of Autoinflammatory Diseases (NCT02974595). Patients or their parents provided written informed consent. Additional written photo consent was obtained from patients included in this manuscript. Most patients were evaluated at the NIH. Patients unable to come to the NIH were consented over the telephone and blood samples for RNA and DNA analysis as well as medical records were sent to the NIH.

**Author Contributions**

AAJ and GAMS acquired data, oversaw the clinical aspects of the study and analyzed data. Members of the Autoinflammatory Diseases Network referred patients and acquired and interpreted clinical data. LM, AB, YH, BM, SM conducted experiments, acquired and analyzed data. SC acquired and analyzed clinical and biomarker subspecialty data. AJO oversaw the statistical analyses of the study data. YH and GAMS acquired clinical data. KRC interpreted clinical and bone marrow biopsy data, SB and ZD analyzed genetic data. AAJ and RGM designed the study, analyzed the data and wrote the first draft of the manuscript. Authors listed in the Autoinflammatory Disease Consortium (AA to TWM) provided critical patient information and phenotyping data. All authors reviewed and approved the final version of the manuscript.

**Acknowledgement**

We would like to thank Samantha Dill, CRNP and Dawn Chapelle, CRNP and Laura Failla, CRNP for excellent patient care, Nicole Plass, Wendy Goodspeed, Michelle O'Brian and

Susan Pfeiffer for scheduling patients. We further thank Paul Wakim for his review and advice on the statistical aspects of the correlation analyses.

**REFERENCES:**

1. de Jesus AA, Canna SW, Liu Y, and Goldbach-Mansky R. Molecular mechanisms in genetically defined autoinflammatory diseases: disorders of amplified danger signaling. *Annual review of immunology.* 2015;33:823-74.
2. Brehm A, Liu Y, Sheikh A, Marrero B, Omoyinmi E, Zhou Q, et al. Additive loss-of-function proteasome subunit mutations in CANDLE/PRAAS patients promote type I IFN production. *The Journal of clinical investigation.* 2015;125(11):4196-211.
3. Liu Y, Jesus AA, Marrero B, Yang D, Ramsey SE, Montealegre Sanchez GA, et al. Activated STING in a vascular and pulmonary syndrome. *The New England journal of medicine.* 2014;371(6):507-18.
4. Bennett L, Palucka AK, Arce E, Cantrell V, Borvak J, Banchereau J, et al. Interferon and granulopoiesis signatures in systemic lupus erythematosus blood. *The Journal of experimental medicine.* 2003;197(6):711-23.
5. Liu Y, Ramot Y, Torrelo A, Paller AS, Si N, Babay S, et al. Mutations in proteasome subunit beta type 8 cause chronic atypical neutrophilic dermatosis with lipodystrophy and elevated temperature with evidence of genetic and phenotypic heterogeneity. *Arthritis and rheumatism.* 2012;64(3):895-907.
6. Yang YG, Lindahl T, and Barnes DE. Trex1 exonuclease degrades ssDNA to prevent chronic checkpoint activation and autoimmune disease. *Cell.* 2007;131(5):873-86.
7. Stetson DB, Ko JS, Heidmann T, and Medzhitov R. Trex1 prevents cell-intrinsic initiation of autoimmunity. *Cell.* 2008;134(4):587-98.
8. Volkman HE, and Stetson DB. The enemy within: endogenous retroelements and autoimmune disease. *Nature immunology.* 2014;15(5):415-22.
9. Crow YJ, Hayward BE, Parmar R, Robins P, Leitch A, Ali M, et al. Mutations in the gene encoding the 3'-5' DNA exonuclease TREX1 cause Aicardi-Goutieres syndrome at the AGS1 locus. *Nature genetics.* 2006;38(8):917-20.
10. Lebon P, Meritet JF, Krivine A, and Rozenberg F. Interferon and Aicardi-Goutieres syndrome. *Eur J Paediatr Neurol.* 2002;6 Suppl A:A47-53; discussion A5-8, A77-86.
11. Sanchez GAM, Reinhardt A, Ramsey S, Wittkowski H, Hashkes PJ, Berkun Y, et al. JAK1/2 inhibition with baricitinib in the treatment of autoinflammatory interferonopathies. *The Journal of clinical investigation.* 2018.
12. Canna SW, de Jesus AA, Gouni S, Brooks SR, Marrero B, Liu Y, et al. An activating NLRC4 inflammasome mutation causes autoinflammation with recurrent macrophage activation syndrome. *Nature genetics.* 2014;46(10):1140-6.
13. Romberg N, Al Moussawi K, Nelson-Williams C, Stiegler AL, Loring E, Choi M, et al. Mutation of NLRC4 causes a syndrome of enterocolitis and autoinflammation. *Nature genetics.* 2014;46(10):1135-9.
14. Bracaglia C, de Graaf K, Pires Marafon D, Guilhot F, Ferlin W, Prencipe G, et al. Elevated circulating levels of interferon-gamma and interferon-gamma-induced chemokines characterise patients with macrophage activation syndrome complicating systemic juvenile idiopathic arthritis. *Annals of the rheumatic diseases.* 2017;76(1):166-72.
15. Weiss ES, Girard-Guyonvarc'h C, Holzinger D, de Jesus AA, Tariq Z, Picarsic J, et al. Interleukin-18 diagnostically distinguishes and pathogenically promotes human and murine macrophage activation syndrome. *Blood.* 2018;131(13):1442-55.

16. Girard-Guyonvarc'h C, Palomo J, Martin P, Rodriguez E, Troccaz S, Palmer G, et al. Unopposed IL-18 signaling leads to severe TLR9-induced macrophage activation syndrome in mice. *Blood.* 2018;131(13):1430-41.
17. Wada T, Kanegane H, Ohta K, Katoh F, Imamura T, Nakazawa Y, et al. Sustained elevation of serum interleukin-18 and its association with hemophagocytic lymphohistiocytosis in XIAP deficiency. *Cytokine.* 2014;65(1):74-8.
18. Gernez Y, de Jesus AA, Alsaleem H, Macaubas C, Roy A, Lovell D, et al. Severe autoinflammation in four patients with C-terminal variants in CDC42 successfully treated with IL-1beta inhibition. *The Journal of allergy and clinical immunology.* 2019.
19. Okamura H, Tsutsi H, Komatsu T, Yutsudo M, Hakura A, Tanimoto T, et al. Cloning of a new cytokine that induces IFN-gamma production by T cells. *Nature.* 1995;378(6552):88-91.
20. Gabay C, Fautrel B, Rech J, Spertini F, Feist E, Kotter I, et al. Open-label, multicentre, dose-escalating phase II clinical trial on the safety and efficacy of tadekinig alfa (IL-18BP) in adult-onset Still's disease. *Annals of the rheumatic diseases.* 2018.
21. Lounder DT, Bin Q, de Min C, and Jordan MB. Treatment of refractory hemophagocytic lymphohistiocytosis with emapalumab despite severe concurrent infections. *Blood Adv.* 2019;3(1):47-50.
22. Gamez-Diaz L, August D, Stepensky P, Revel-Vilk S, Seidel MG, Noriko M, et al. The extended phenotype of LPS-responsive beige-like anchor protein (LRBA) deficiency. *The Journal of allergy and clinical immunology.* 2016;137(1):223-30.
23. Esposito DL, Li Y, Vanni C, Mammarella S, Veschi S, Della Loggia F, et al. A novel T608R missense mutation in insulin receptor substrate-1 identified in a subject with type 2 diabetes impairs metabolic insulin signaling. *The Journal of clinical endocrinology and metabolism.* 2003;88(4):1468-75.
24. Esposito DL, Mammarella S, Ranieri A, Della Loggia F, Capani F, Consoli A, et al. Deletion of Gly723 in the insulin receptor substrate-1 of a patient with noninsulin-dependent diabetes mellitus. *Human mutation.* 1996;7(4):364-6.
25. German JP, Wisse BE, Thaler JP, Oh IS, Sarruf DA, Ogimoto K, et al. Leptin deficiency causes insulin resistance induced by uncontrolled diabetes. *Diabetes.* 2010;59(7):1626-34.
26. Lo B, Zhang K, Lu W, Zheng L, Zhang Q, Kanellopoulou C, et al. AUTOIMMUNE DISEASE. Patients with LRBA deficiency show CTLA4 loss and immune dysregulation responsive to abatacept therapy. *Science.* 2015;349(6246):436-40.
27. Leshinsky-Silver E, Malinger G, Ben-Sira L, Kidron D, Cohen S, Inbar S, et al. A large homozygous deletion in the SAMHD1 gene causes atypical Aicardi-Goutieres syndrome associated with mtDNA deletions. *European journal of human genetics : EJHG.* 2011;19(3):287-92.
28. de Jesus AA, Brehm A, VanTries R, Pillet P, Parentelli AS, Montealegre Sanchez GA, et al. Novel proteasome assembly chaperone mutations in PSMG2/PAC2 cause the autoinflammatory interferonopathy CANDLE/PRAAS4. *The Journal of allergy and clinical immunology.* 2019;143(5):1939-43 e8.
29. Rice G, Newman WG, Dean J, Patrick T, Parmar R, Flintoff K, et al. Heterozygous mutations in TREX1 cause familial chilblain lupus and dominant Aicardi-Goutieres syndrome. *American journal of human genetics.* 2007;80(4):811-5.
30. Buchbinder D, Montealegre Sanchez GA, Goldbach-Mansky R, Brunner H, and Shulman AI. Rash, Fever, and Pulmonary Hypertension in a 6-Year-Old Female. *Arthritis care & research.* 2018;70(5):785-90.

31. Kuemmerle-Deschner JB, Verma D, Endres T, Broderick L, de Jesus AA, Hofer F, et al. Clinical and Molecular Phenotypes of Low-Penetrance Variants of NLRP3: Diagnostic and Therapeutic Challenges. *Arthritis Rheumatol.* 2017;69(11):2233-40.
32. Kanda N, Shimizu T, Tada Y, and Watanabe S. IL-18 enhances IFN-gamma-induced production of CXCL9, CXCL10, and CXCL11 in human keratinocytes. *European journal of immunology.* 2007;37(2):338-50.
33. Sanchez GAM, Reinhardt A, Ramsey S, Wittkowski H, Hashkes PJ, Berkun Y, et al. JAK1/2 inhibition with baricitinib in the treatment of autoinflammatory interferonopathies. *The Journal of clinical investigation.* 2018.
34. Kim H, de Jesus AA, Brooks SR, Liu Y, Huang Y, VanTries R, et al. Development of a Validated Interferon Score Using NanoString Technology. *Journal of interferon & cytokine research : the official journal of the International Society for Interferon and Cytokine Research.* 2018;38(4):171-85.
35. Konig N, Fiehn C, Wolf C, Schuster M, Cura Costa E, Tungler V, et al. Familial chilblain lupus due to a gain-of-function mutation in STING. *Annals of the rheumatic diseases.* 2017;76(2):468-72.
36. Fremond ML, Rodero MP, Jeremiah N, Belot A, Jeziorski E, Duffy D, et al. Efficacy of the Janus kinase 1/2 inhibitor ruxolitinib in the treatment of vasculopathy associated with TMEM173-activating mutations in 3 children. *The Journal of allergy and clinical immunology.* 2016;138(6):1752-5.
37. Meesilpavikkai K, Dik WA, Schrijver B, van Helden-Meeuwsen CG, Versnel MA, van Hagen PM, et al. Efficacy of Baricitinib in the Treatment of Chilblains Associated With Aicardi-Goutieres Syndrome, a Type I Interferonopathy. *Arthritis Rheumatol.* 2019;71(5):829-31.
38. Vanderver A. *2017 American Academy of Neurology*. Boston, MA, USA; 2017.
39. Lopez-Herrera G, Tampella G, Pan-Hammarstrom Q, Herholz P, Trujillo-Vargas CM, Phadwal K, et al. Deleterious mutations in LRBA are associated with a syndrome of immune deficiency and autoimmunity. *American journal of human genetics.* 2012;90(6):986-1001.
40. Wessel AWH, A.P.; Zilberman-Rudenko, J.; Goldbach-Mansky, R.; Siegel, R.M.; Hanson, E.P. . Inflammatory disease and an impaired type I interferon response resulting from a de novo human NEMO hypomorphic mutation. *Arthritis and Rheumathology Abstract Supplement 2013 Annual Meeting.* 2013;65(10 (Supplement)):S323.
41. Tesi B, Davidsson J, Voss M, Rahikkala E, Holmes TD, Chiang SCC, et al. Gain-of-function SAMD9L mutations cause a syndrome of cytopenia, immunodeficiency, MDS, and neurological symptoms. *Blood.* 2017;129(16):2266-79.
42. Nagata Y, Narumi S, Guan Y, Przychodzen BP, Hirsch CM, Makishima H, et al. Germline loss-of-function SAMD9 and SAMD9L alterations in adult myelodysplastic syndromes. *Blood.* 2018;132(21):2309-13.
43. Pastor VB, Sahoo SS, Boklan J, Schwabe GC, Saribeyoglu E, Strahm B, et al. Constitutional SAMD9L mutations cause familial myelodysplastic syndrome and transient monosomy 7. *Haematologica.* 2018;103(3):427-37.
44. Chen DH, Below JE, Shimamura A, Keel SB, Matsushita M, Wolff J, et al. Ataxia-Pancytopenia Syndrome Is Caused by Missense Mutations in SAMD9L. *American journal of human genetics.* 2016;98(6):1146-58.
45. Ichida H, Kawaguchi Y, Sugiura T, Takagi K, Katsumata Y, Gono T, et al. Clinical manifestations of Adult-onset Still's disease presenting with erosive arthritis: Association with low levels of ferritin and Interleukin-18. *Arthritis care & research.* 2014;66(4):642-6.

46. Mazodier K, Marin V, Novick D, Farnarier C, Robitail S, Schleinitz N, et al. Severe imbalance of IL-18/IL-18BP in patients with secondary hemophagocytic syndrome. *Blood.* 2005;106(10):3483-9.
47. Shimizu M, Nakagishi Y, and Yachie A. Distinct subsets of patients with systemic juvenile idiopathic arthritis based on their cytokine profiles. *Cytokine.* 2013;61(2):345-8.
48. Schulert GS, Yasin S, Carey B, Chalk C, Do T, Schapiro AH, et al. Systemic Juvenile Idiopathic Arthritis-Associated Lung Disease: Characterization and Risk Factors. *Arthritis Rheumatol.* 2019.
49. Wunderlich M, Stockman C, Devarajan M, Ravishankar N, Sexton C, Kumar AR, et al. A xenograft model of macrophage activation syndrome amenable to anti-CD33 and anti-IL-6R treatment. *JCI Insight.* 2016;1(15):e88181.
50. Suzuki T, and Trapnell BC. Pulmonary Alveolar Proteinosis Syndrome. *Clinics in chest medicine.* 2016;37(3):431-40.
51. Bohn E, Sing A, Zumbihl R, Bielfeldt C, Okamura H, Kurimoto M, et al. IL-18 (IFN-gamma-inducing factor) regulates early cytokine production in, and promotes resolution of, bacterial infection in mice. *J Immunol.* 1998;160(1):299-307.
52. Sin JH, and Zangardi ML. Ruxolitinib for secondary hemophagocytic lymphohistiocytosis: First case report. *Hematol Oncol Stem Cell Ther.* 2017.
53. Broglie L, Pommert L, Rao S, Thakar M, Phelan R, Margolis D, et al. Ruxolitinib for treatment of refractory hemophagocytic lymphohistiocytosis. *Blood Adv.* 2017;1(19):1533-6.
54. Zandvakili I, Conboy CB, Ayed AO, Cathcart-Rake EJ, and Tefferi A. Ruxolitinib as first-line treatment in secondary hemophagocytic lymphohistiocytosis: A second experience. *American journal of hematology.* 2018;93(5):E123-E5.
55. Prencipe G, Bracaglia C, and De Benedetti F. Interleukin-18 in pediatric rheumatic diseases. *Current opinion in rheumatology.* 2019;31(5):421-7.

**TABLES**

**Table 1. Clinical features of genetically defined Type-I interferonopathies and non-interferonopathies**

| | Clinical Feature | With IFN signature Affected / no. patients evaluated (%) n=41[A] | Without IFN signature Affected / no. patients evaluated (%) n=25 | Fisher exact test p-value |
|---|---|---|---|---|
| Demographics | ***Age of disease onset ((Median (IQ range)), months***[B] | 6 (0 - 15) | 24 (1.5 - 57) | ***0.009***[G] |
| | ***Age of disease onset < 2yrs*** | 31 / 41 (75) | 12 / 25 (48) | ***0.033*** |
| | **Female Gender** | 24 / 41 (58) | 11 / 25 (44) | ns |
| | ***White Race*** | 21 / 41 (51) | 21 / 25 (84) | ***0.009*** |
| | ***Mortality***[C] | 8 / 41 (19.5) | 0 / 25 (0) | ***0.020*** |
| Skin | ***Any rash*** | 37 / 39 | 17 / 25 | ***0.010*** |
| | ***Panniculitis with or without lipodystrophy*** | 22 / 41 (54) | 0 / 25 (0) | ***<0.0001*** |
| | **Pustulosis** | 2 / 41 (5) | 3 / 25 (12) | ns |
| | **Pyoderma gangrenosum** | 1 / 41 (2.4) | 1 / 25 (4) | ns |
| Neurologic | ***Basal ganglia calcifications*** | 12 / 26 (46) | 0 / 14 (0) | ***0.003*** |
| | **Demyelinating disease**[D] | 7 / 25 (28) | 1 / 14 (7) | ns |
| | **Aseptic meningitis**[E] | 3 / 28 (11) | 1 / 22 (4.5) | ns |
| Pulmonary | ***Interstitial lung disease with or without clubbing***[F] | 18 / 38 (47) | 1 / 19 (5.3) | ***0.002*** |
| Musculoskeletal | ***Myositis***[H] | 21 / 35 (60) | 2 / 19 (10) | ***0.0005*** |
| | ***Aseptic osteomyelitis*** | 1 / 40 (2.5) | 6 / 19 (32) | ***0.010*** |
| Vascular | **Skin vasculitis** | 10 / 40 (25) | 2 / 25 (8) | ns |
| | **Stroke** | 2 / 37 (5.4) | 1 / 25 (4) | ns |
| | ***Arterial hypertension*** | 10 / 33 (30) | 1 / 25 (4) | ***0.016*** |
| | **Vascular calcification** | 5 / 33 (15) | 0 / 19 (0) | ns |
| Liver disease | ***Transaminitis*** | 23 / 38 (61) | 3 / 25 (12) | ***0.0002*** |
| | **Abnormal liver biopsy**[I] | 7 / 38 (16) | 1 / 25 (4) | ns |
| Other | **MAS** | 11 / 39 (28) | 2 / 25 (8) | 0.062 |

[A] For clinical phenotyping, 4 patients (G1-P3, G1-P5, G4-P3 and G4-P6) were negative and 1 patient (G4-P5) did not have an interferon (IFN) response gene score (IRG-S) tested but were later added the respective groups when clinical or genetic diagnosis was made. The final number

of subjects in the group of patients with a diagnosis related to a “positive” IRG-S (with IFN signature) was 41, and 25 patients were listed with “negative” IRG-S (without IFN signature).
[B] 2 patients in this group had disease onset above 18 years old and were excluded from the analysis
[C] One patient with SAMD9L-associated autoinflammatory disease (SAMD9L-SAAD) was diagnosed post-mortem (G4-P5)
[D] Patients with magnetic resonance imaging (MRIs)
[E] Patients with lumbar puncture (LP)
[F] Patients with chest computed tomography (CTs)
[G] Unpaired t-test was performed
[H] Myositis was defined as elevated creatine kinase (CK) or aldolase and/or abnormal muscle MRI
[I] Undifferentiated interferonopathies (UIFN) group: histiocytes infiltration (n=1)(G1-P3); granulomatous hepatitis (n=2)(G2-P1 and G3-P1); autoimmune hepatitis with liver fibrosis (n=1)(G2-P2); nodular regenerative hyperplasia (n=1)(G5-P3); ballooning and necrosis of hepatocytes (n=2)(G6-P1 and G6-P2) and periportal fibrosis (n=1)(G6-P1). Non-interferonopathies (NonIFN) group: liver fibrosis and vanishing bile duct disease (n=1) (GN5-P3). Features italicized and underlined were significantly different between patients with and without IFN signatures.

**Table 2. Diagnoses of patients with elevated Type-1 IFN scores (IRG-S), including genetic and immune evaluation**

| Disease group | Number of patients in group (n=41) | Disease name | Number of patients with monogenic disease-causing mutation | Presumed genetic mechanism | Possible candidate/modifying genes | Diagnostic approach to a clinical diagnosis [E] |
|---|---|---|---|---|---|---|
| Group 1 | n=8 | **IL-18 PAP-MAS** | **n=0[A]** | poly/oligogenic | none/possible modifying genes | Clinical phenotype and cytokine analysis (high IL-18) |
| Group 2 | n=2 | **LRBA deficiency** | **n=2[B]** | ***LRBA*** *compound heterozygous,* recessive | monogenic/modifying genes | Genetic testing (WES) |
| Group 3 | n=4 | **NEMO-NDAS** | **n=4** | ***IKBKG*** encoding NEMO, novel splice site mutations, X-linked | monogenic/none | Genetic testing (WGS) |
| Group 4 | n=6 | **SAMD9L-SAAD** | **n=6[C]** | ***SAMD9L****,* de novo frameshift mutations, autosomal dominant | monogenic/none | Genetic testing (WES), trio analysis |
| Group 5 | n=4 | **AGS/AGS-like** | **n=1** | ***SAMHD1****,* recessive | 1 candidate gene/NA | Genetic testing (WGS) |
| Group 6 | n=2 | **MYOSITIS + positive anti-MDA5 autoantibody** | **n=0** | not known | none/possible modifying genes | Clinical phenotype and autoantibody testing |
| Group 7 | n=6 | **CANDLE/CANDLE-LIKE WITH PANNICULITIS** | **n=4[D]** | ***PSMB8 recessive (n=2); PSMG2*** recessive (n=1); ***TREX1*** de novo, somatic (n=1) | 2 candidate genes/NA | Genetic testing (WES), trio analysis |
| Group 8 | n=2 | **SAVI-like** | **n=0** | not known | none/no modifying genes | Clinical phenotyping |
| Group 9 | n=7 | **Miscellaneous** | **n=1** | variable, not one disease | possible candidates/NA | Clinical phenotyping |

[A] One patient was diagnosed with myeloid leukemia after treatment for MAS that included etoposide.

[B] Both patients have modifying genes that may influence their phenotype

[C] One patient was included post-mortem because of a disease-causing *SAMD9L* mutation that was identical to two other patients

[D] 3 patients have novel proteasome mutations and have CANDLE/PRAAS, one patient had a known *PSMB8* mutation, p.T75M

[E] See Supplemental Table 7 for best candidate genes

**FIGURES**

Figure 1.

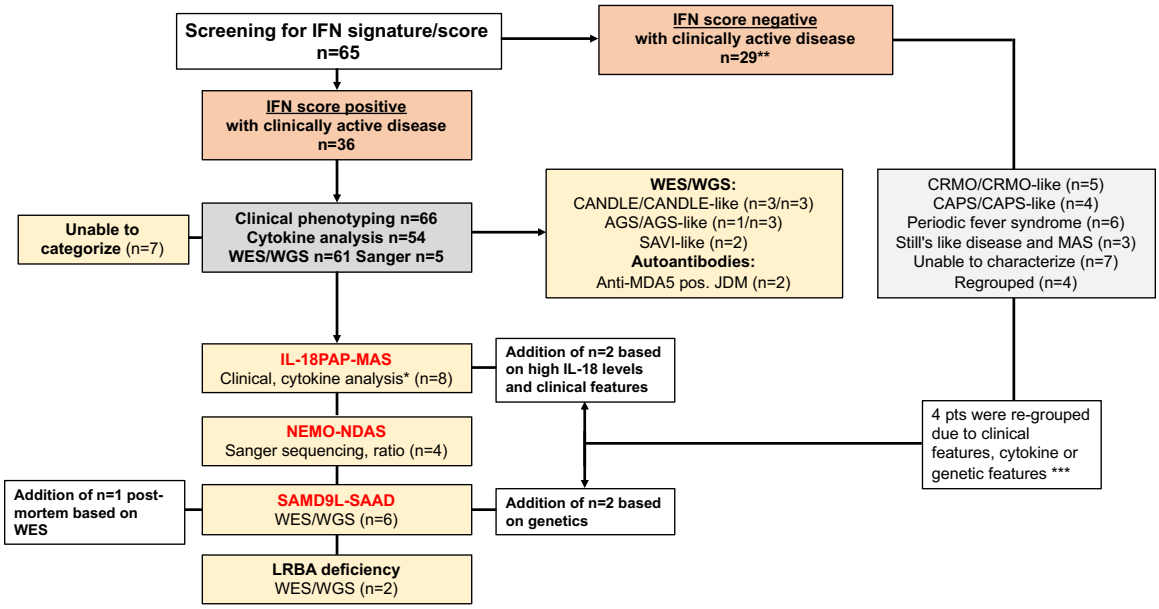


**Figure 1. Study overview, patient allocation and diagnosis.** All patients were screened for elevation of an IFN response gene score (IRG-S) except for one patient (G4P5), who post-mortem was diagnosed based on WES with SAMD9L-SAAD. Patients were characterized based on presence or absence of an IRG-S. All patients underwent clinical phenotpying, cytokine analyses and genetic testing (WES/WGS or Sanger sequencing). IFN score negative patients were clinically grouped (see supplement). IFN score positive patients were grouped as CANDLE-like, SAVI like and AGS like disease. Cytokine analyses and genetic analyses allowed for the characterization of patients with 3 additional diseases: IL-18PAP-MAS, NEMO-NDAS, SAMD9L-SAAD (in red) and 2 patients had LRBA deficiency. Three patients had CANDLE, 1 AGS5 and 2 were MDA5 autoantibody positive. 7 patients with an IFN signature and 7 patients without an IFN signature could not be further classified. *No monogenic candidate gene. **IFN score negative patients were classified as: CRMO/CRMO-like (n=5); CAPS/CAPS-like (n=4), Periodic fever syndrome (n=6), Still's like disease and MAS (n=3); 7 patients could not be classified. ***2 patients (G1P5, G4P6) only had one sample, 1 patient, (G4P3) had a bone marrow transplant (BMT) and no pre-BMT sample available, one patient had 3 negative samples (G1P3).

Figure 2.

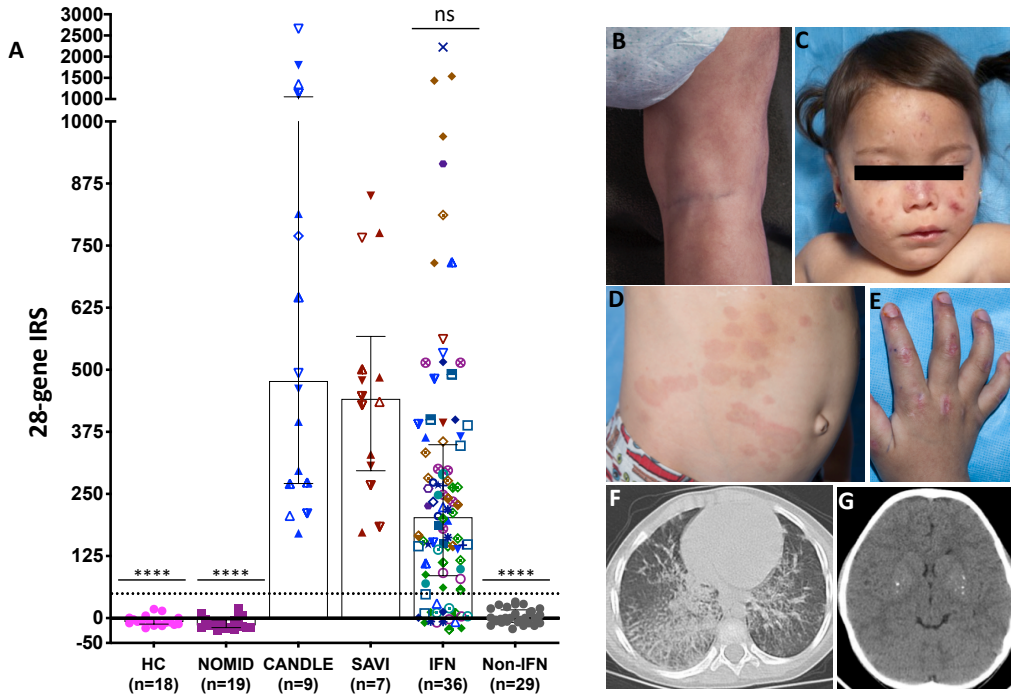


**Figure 2. Shared clinical features and different cytokine profiles in patients with and without elevated IFN scores.** (**A**) An elevated IFN score distinguishes 36 patients during active disease from 29 patients who had normal IFN scores during bouts of active disease. Nonparametric (Kruskal-Wallis) test was used for multiple comparisons of IFN or Non-IFN groups with healthy controls (HC) or with CANDLE and SAVI patients combined. Depicted in the graph are the statistical significances (Kruskal-Wallis test) from the comparisons of each group (NOMID, IFN and Non-IFN groups) with CANDLE and SAVI patients combined. Each individual patient is represented by a different symbol shape. **** $p<0.0001$, ns: not significant. Bars and error lines indicate median and interquartile range, respectively; dotted line indicates the 28-gene IFN score cutoff (48.9) previously described (34). Multiple comparisons of each group (NOMID, CANDLE and SAVI combined, IFN and Non-IFN) with HC (not depicted): NOMID p=0.5004, CANDLE+SAVI *p<0.0001*, IFN *p<0.0001*, Non-IFN p=0.2986. For HC, NOMID and non-IFN groups, the same symbol is used for different individuals as only one sample per patient is included. For CANDLE, SAVI and IFN groups, each patient is represented by a different symbol. (**B**-**G**) Characteristic clinical features that were present only in patients with elevated IFN scores included panniculitis with lipoatrophy (**B**), neutrophilic vasculitis (**C**), erythematous macular rash (**D**), Gottron's papules (**E**), interstitial lung disease (**F**), basal ganglia calcifications (**G**). Four patients (per groups defined in Table 2, Group 1 – Patient 3 or G1-P3 and G1-P5, G4-P2 and G4-P5) had negative IRG-S but were later added to the respective groups when a clinical or genetic diagnosis was made (not depicted).

Figure 3.

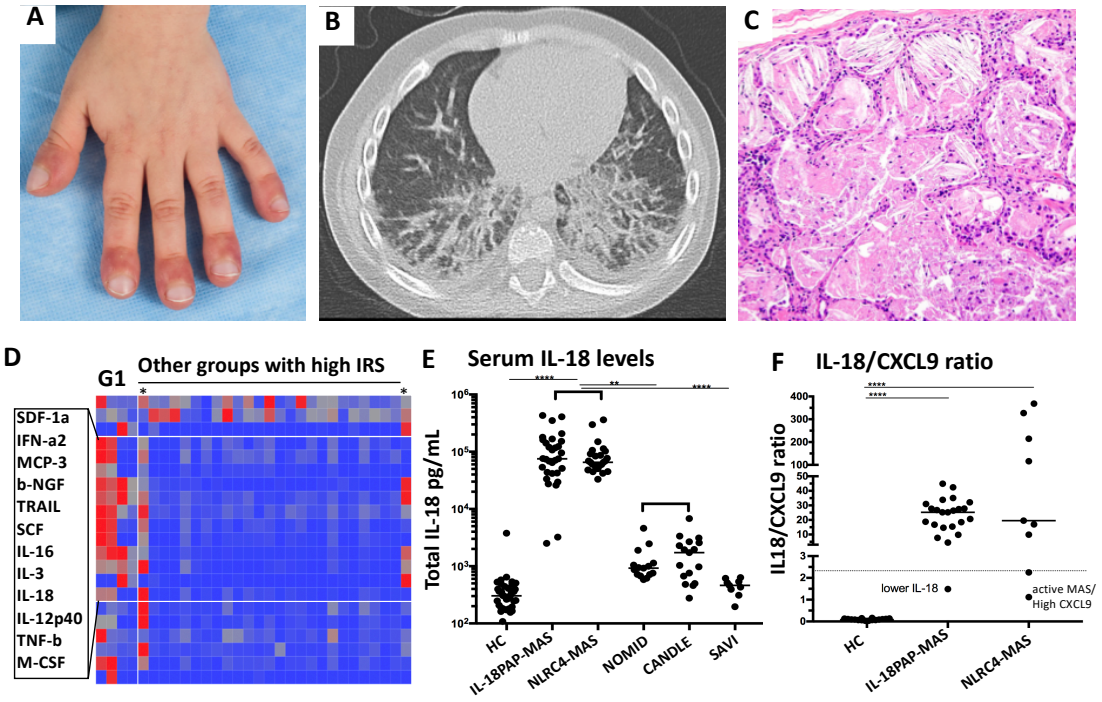


**Figure 3. Clinical features and cytokine dysregulation in patients with IL-18PAP-MAS** (n=8) (**A**) Nail clubbing (**B**) Interstitial and alveolar lung disease (**C**) Histologic features characteristic of pulmonary alveolar proteinosis. Magnification is 20x. (**D**) Heatmap of 22 out of 48 analytes tested. The 12-cytokine signature includes SDF-1α/CXCL12, IFN-α2, MCP-3/CCL7, β-NGF, TRAIL, SCF, IL-16, IL-3, IL-18, IL-12p40, TNF-β/Lt α and M-CSF. The 12-cytokine signature upregulation tracks with ultra-high IL-18 levels that are also seen in patients with recurrent macrophage activation syndrome (MAS) and gain-of-function mutations in *NLRC4* (12). Two other patients with the 12-cytokine signature (*) had MAS but no pulmonary disease. (**E**) Serum IL-18 levels in patients with IL-18PAP-MAS and healthy and disease controls. HC= healthy controls, IL-18PAP-MAS= G1 patients with pulmonary alveolar proteinosis (PAP) and recurrent MAS (n=8), NLRC4/MAS= patients with monogenic NLRC4 mediated MAS (n=5), NOMID= neonatal-onset multisystem inflammatory disease (n=8), SAVI= STING associated vasculopathy with onset in infancy (n=5), CANDLE= chronic atypical neutrophilic dermatosis with lipodystrophy and elevated temperatures (n=8). (**F**) IL-18/CXCL9 ratio has previously been described to cut off of 2.3 (15) is indicated with a gray horizontal line. IL-18PAP-MAS (n=7); NLRC4/MAS= patients with monogenic NLRC4 mediated MAS (n=5). (**E**, **F**) Nonparametric test (Kruskal-Wallis) was performed for multiple comparisons and all significant differences are shown. In **E**, populations in brackets share the same significance pattern. *p<0.05, **p<0.01, ***p<0.001, ****p<0.0001.

Figure 4.

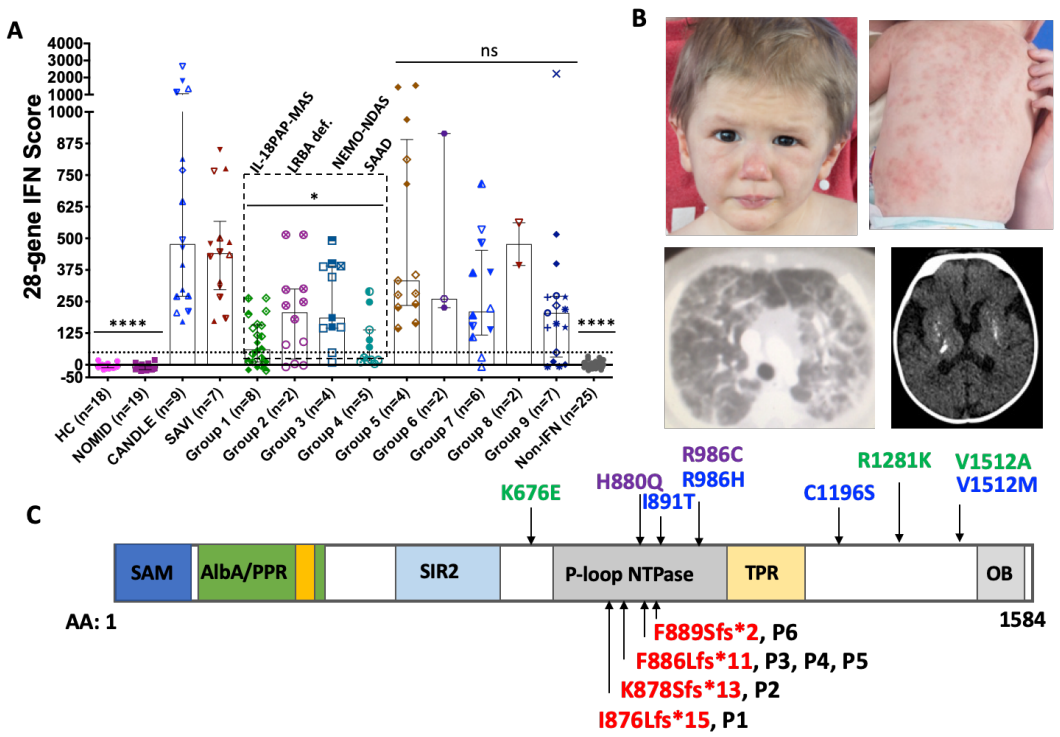


**Figure 4. IFN score by disease group and clinical and genetic characteristics of SAMD9L-mediated autoinflammatory disease (SAMD9L-SAAD)** (**A**) 28-gene IFN scores by disease group. Nonparametric tests were used for multiple comparisons (Kruskal-Wallis) or individual group comparisons (Mann-Whitney). Each patient in groups 1 to 9 (G1 to G9) is represented by a different symbol shape. Depicted in the graph are the statistical significances (Kruskal-Wallis test) from the comparisons of each group (HC, NOMID, G1 to G4 combined, G5, G6, G7, G8, G9 and Non-IFN groups) with CANDLE and SAVI patients combined. * *p=0.0259*, **** *p<0.0001*, ns: not significant. Bars and error lines indicate median and interquartile range, respectively; dotted line indicates the 28-gene IFN score cutoff (48.9) previously described (34). For the control groups, HC and NOMID, the same symbol is used for different individuals as only one sample per patient is included. For all other disease groups including CANDLE and SAVI, each patient is represented by a different symbol. (**B**) Clinical manifestations of SAMD9L-associated autoinflammatory disease (SAMD9L-SAAD) include nodular panniculitis and lipoatrophy (patient 1), interstitial lung disease (patient 3), basal ganglia calcifications (patient 5) (**C**) SAMD9L domains and variant localization: SAM (blue): Sterile α motif domain, AlbA/PPR (orange/yellow): DNA-binding domain, SIR2 (light blue): silent mating-type information regulator 2, P-loop NTPase (green): P-loop-containing NTP hydrolase, TPR (purple): tetratricopeptide repeat domain, OB (gray): oligonucleotide-binding fold domain, AA: amino acid, P1-P6: patient 1 to patient 6. Variants identified in SAMD9L-SAAD are in red, variants associated with ataxia-pancytopenia syndrome (APS) are in blue and variants associated with myelodysplastic syndrome (MDS) or acute myeloid leukemia (AML) are in green. Variants associated with either APS or MDS/AML are shown in purple.

Figure 5.

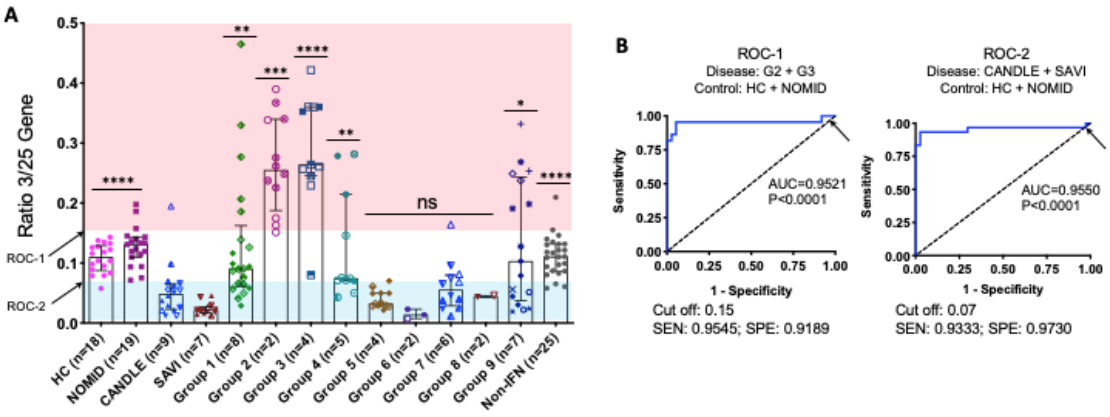


**Figure 5. Ratios of 3-gene score (CXCL10+GBP1+SOCS1) over 25-gene score (3/25 gene ratio).** (**A**) A ratio between 3-IFN response genes with NF-κB transcription binding sites (CXCL10, GBP1 and SOCS1) and the 25-IFN genes with no NF-κB binding sites (3/25 ratio) was calculated. Depicted in the graph are the statistical significances (nonparametric Kruskal-Wallis test) from the comparisons of each group with CANDLE and SAVI patients combined: HC and NOMID combined *p<0.0001*, G1 *p=0.0017*, G2 *p=0.0003*, G3 *p<0.0001*, G4 *p=0.0027*, G5 p=0.9271, G6 p=0.6055, G7 p=0.1499, G8 p=0.8684, G9 p=0.0083, Non-IFN *p<0.0001*. ns: not significant. Bars and error lines indicate median and interquartile range, respectively. Red shade area indicates a high 3/25-gene ratio, blue shade area indicates low ratio and white area indicates normal ratio. Cut offs were calculated in panel B. For the control groups (HC, NOMID) the same symbol is used for different individuals as only one sample per patient is included. In all other groups, including CANDLE and SAVI, each patient is represented by a different symbol. (**B**) Two Receiver Operating Characteristic (ROC) curves for the 3/25 gene ratio to distinguish HC and NOMID from patients with NDAS (G3) and LRBA deficiency (G2) (ROC-1) and CANDLE and SAVI from HC and NOMID (ROC-2) are shown. A black arrow indicates the optimal cut off (listed under each graph). AUC: area under the curve; SEN: sensitivity; SPE: specificity. The cut offs for the ROC curves were marked in panel A with black arrows on the Y axis. A list of genes in the IFN-gene score is published in ref. 34.